Scooturbine: A Recycled Wind Generator Blade Design report

Sam Griffen
Submitted for ENGR440

I. Introduction

One of the most important aspects of a wind turbine is the efficiency with which energy can be extracted from the wind. A large part of this efficiency depends on the aerodynamic properties and configuration of the blades. It is therefore critical that any turbine design considers the impact of all relevant blade parameters, and implements some process to optimise aerodynamic efficiency.

This report proposes a process for designing blades for *Scooturbine* and analysing their potential effectiveness. A catalog of potential airfoils is developed, and each foil is analysed in QBlade. Simulation results are utilised to select the three most optimal airfoils for the application. These airfoils are used to generate 3D blade models for fabrication and attachment to the developed nacelle.

II. Background

A. Important Terminology

1) Airfoil Concepts: Airfoils are shapes designed to generate lift as they travel through a fluid. Blade cross section is always based on some airfoil design, chosen to provide optimal lift based on various aerodynamic parameters. An in depth discussion of aerodynamics and how this lift is generated is out of scope for this project, however understanding basic parameters in order to compare airfoil effectiveness is critical.

Figure 1 summarises the important parameters of an airfoil, showing a two dimensional cross section of a blade [1]. A single blade is made up of a number of sections of airfoil, and parameters vary along the blade to optimise efficiency.

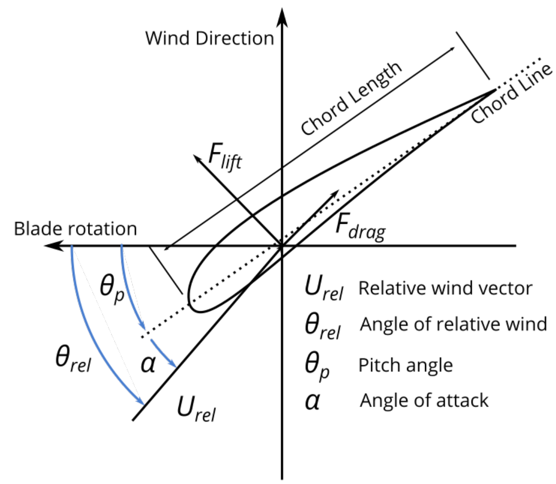

Fig. 1: Blade airfoil parameter diagram. Adapted from *Wind Energy Explained* [1]

On a turbine blade the chord, defined as the line from leading tip to the trailing tip, is not parallel with the wind velocity. Due to the rotation of the rotor the airflow passing over the blade is a combination of the oncoming wind and the relative air velocity in the plane of rotation. These vectors sum to give the resultant wind vector, U_{rel} in the diagram. U_{rel} passing over the airfoil results in the lift force, F_L. A given airfoil will have an optimal angle of attack, α, which combined with θ_{rel} will give an optimal pitch angle θ_p.

Finally, when analysing airfoils it is important to understand the concept of glide ratio. Airfoils are often analysed based on their coefficient of lift (C_l) and coefficient of drag (C_d), which are quantifiers representing how significant each force is on the airfoil. It is desirable to have high lift, and low drag. Glide ratio refers to the lift to drag ratio $\frac{C_l}{C_d}$, and maximising this ratio gives optimal performance.

2) Reynolds Number: Reynolds number is a dimensionless value quantifying the ratio between "inertial" and "viscous" forces in a flowing fluid [1]. Viscous force describes the shear forces due to relative motion of layers within a fluid, while inertial force describes forces due to the momentum of the fluid . In depth understanding of fluid dynamics is not required for this project, and Reynolds number is used at a very high level.

Effectively Reynolds number describes how laminar or turbulent a flow will be, and is frequently used for modelling and simulation of aerodynamic systems. Equation 1 shows how it is calculated in the context of wind turbine blades [1]. The characteristic length L is a length that gives scale to the flow, and in this case the chord length is used. Kinematic viscosity is a property of the air, and is defined as approximately 1.5×10^{-5} at standard conditions of $\approx 20°\text{C}$, and one atmosphere [2].

$$Re = \frac{UL}{v} \quad (1) \quad \begin{aligned} U &= \text{Velocity of flow} \\ L &= \text{Characteristic length} \\ v &= \text{Kinematic viscosity} \end{aligned}$$

In the context of wind turbines, the Reynolds number can be thought of as a quantity that describes the scale of the air flow at the blade, and is primarily useful for simulation of blade components.

3) Tip Speed Ratio: Tip speed ratio (TSR) is a measure of the velocity of the blade tip relative to the wind velocity. TSR is calculated as shown in Equation 2 [3].

$$\lambda = \frac{\Omega R}{U} = \frac{V_{tip}}{V_{wind}} \quad (2) \quad \begin{aligned} \Omega &= \text{Angular velocity} \\ R &= \text{Blade radius} \\ U &= \text{Wind velocity} \end{aligned}$$

4) Available Power & Betz's Limit: When designing a turbine, it is important to identify how much power is available to the turbine in the first place. Equation 3 may be used to calculate the kinetic energy in the air that is passing through the rotor [3].

$$P = \frac{\rho A V^3}{2} \quad (3) \quad \begin{aligned} P &= \text{Available power} \\ \rho &= \text{Air density} \\ A &= \text{Swept area} \\ V &= \text{Wind velocity} \end{aligned}$$

However, this is not an indication of the maximum power the generator can potentially generate. If the turbine were 100% efficient, the wind would need to be stopped completely by the rotor, which would not be possible as this would result in no aerodynamic forces. This is the concept behind the Betz limit, which states that a theoretically ideal turbine can only extract 59.3% of the kinetic energy [1]. This is a theoretical maximum limit and is likely to not be achieved due to additional aerodynamic losses, as well as mechanical and electrical losses. However, this does provide a useful upper limit on the turbine power output potential.

B. Existing Work

Existing work has been reviewed in order to identify key considerations when designing a wind turbine on such a small scale. The goal of this review is to identify key parameters, potential problems, and potential design processes.

In their 1997 paper *Low Reynolds Number Airfoils for Small Horizontal Axis Wind Turbines*, P. Giguere and M. Selig develop guidelines for selecting airfoils for small horizontal axis wind turbines (HAWT) [4]. They make the point that these small turbines operate at very low Reynolds numbers, and if an airfoil designed for this application is not selected the abnormal aerodynamics can severely limit the performance. One of the biggest issues with low Reynolds number operation is the formation of a "laminar seperation bubble" on the blade. They comment that low Reynolds number airfoils are designed to minimise the drag resulting from this bubble, and as such are very relevant in small turbine design. With this in mind, the paper analyses a database of 15 low Reynolds number air foils.

With analysis of each airfoil performed, a set of guidelines for selecting airfoils is presented. Two main types of turbine are discussed; variable speed, and variable pitch, each with their own set of considerations. Variable speed turbines maintain a constant

TSR, resulting in the rotor velocity changing with wind speed. Variable pitch turbines are what is often seen in larger installations, with a mechanism to vary blade pitch and maintain constant rotor velocity. Variable speed turbines are of particular interest for this project, as a blade pitching mechanism will not be developed.

It is highlighted that variable speed turbines ideally operate at constant TSR, making optimisation of blade section pitch relatively straightforward. This leads to airfoil selection relying primarily on maximum glide ratio characteristics.

Much of the modern work around small turbine optimisation identifies the fact that there are many variables at play, and employs simulation aided methods to produce optimal results. A good example of this is the 2019 paper *Small Wind Turbine Blade Design and Optimization*, which details a heavily simulation based method for iterating on blade designs [5]. This paper identifies that many of the parameters of a wind turbine blade are heavily interdependent. To approach this the study developed a script for iterating on a design via Blade Element Momentum (BEM) analysis. Along with this, the software package QBlade is utilised for more in depth simulation of both airfoils and entire turbine characteristics.

III. Location Analysis

Turbine design is very reliant on the intended installation location, as turbine parameters are based on average wind conditions and factors such as allowed space for installation. This project aims to develop a turbine for installation on a fenceline attached to a greenhouse, in order to provide energy to a lighting, irrigation, and heating system within the greenhouse. This fenceline is at the top of a high bank, with an unobstructed view north.

Figure 2 shows a view from the road at the base of the bank, looking up to the installation location. It is worth noting that this location is on the northside of a household, and therefore only northerly winds will provide energy to the generator. Figure 3 shows the view from the greenhouse, looking north. This highlights the almost completely unobstructed view. It is worth noting that the tree in the right of Figure 3 is currently the only obstruction, however many of the branches are dead or dying, and it is not expected to remain on the bank into the future.

Fig. 2: View of installation location from road. Intended installation location highlighted red.

Fig. 3: View of installation location from greenhouse, looking north.

With a specific installation location identified, typical windspeed information has been obtained via the NIWA Solarview tool [6]. This information has been processed to obtain a windspeed distribution curve, shown in Figure 4. Initially, this plot shows an average windspeed between 6 and 8 ms^{-1}. Further analysis showed this to result in an average windspeed of 7.08 ms^{-1}. The plot also exhibits interesting behaviour around the lower windspeed values. Windspeed is expected to approximately follow a Weibull distribution [7], and this is generally true of the generated plot. However the frequency of speeds between 0 and 2 ms^{-1} appears slightly higher than would be expected. This indicates skew towards lower windspeeds, potentially requiring a low cut-in speed.

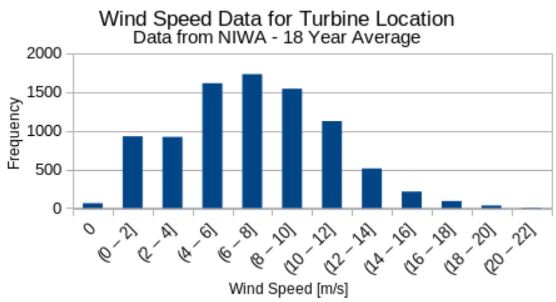

Fig. 4: Windspeed distribution over 18 year period for chosen location. Data from NIWA [6]

It is worth noting that this data does not tell the whole story, as it is averaged over 18 years, and it is not measured at the site of the turbine. It is likely calculated based on data from a range of nearby weather measurement stations, and therefore does not show any irregularities present at the actual location.

One of the biggest factors that is not represented is the fact that given the position of the turbine on the north side of the building only northerlies provide energy. Oberservation of the location over a number of years suggests that this is a frequent occurance, however there is no data to verify this. Ideally, an anemometer would be set up to measure data for a long time period, providing a detailed idea of wind speed and direction behaviour in the location of the turbine. An anemometer system is being developed for future iterations of this design.

IV. Design

As highlighted in a large portion of the literature, wind turbine optimisation is often an iterative process, utilising software approaches to converge on an effective result. This section outlines such a design process, producing a small number of blade candidates for physical testing.

At a high level, the design process has the following outline:

- Determine environmental/physical limitations, and requirements.
- Make initial design decisions on parameters that will not vary with airfoil decisions. This includes TSR and blade count.
- Develop a catalogue of potential airfoils. Existing work in the field is used to identify effective low Reynolds number airfoils.
- Iteratively determine the predicted Reynolds number for each airfoil.
- Generate lift polars via QBlade simulation.
- Identify three airfoils for fabrication and physical analysis based on maximum glide ratio, and optimal drag bucket formation.
- Produce 3D models for each blade.

A. Requirements & Initial Design Specifications

As discussed previously, the turbine must fit into a relatively confined area. The turbine is to be mounted at the top of a high bank, with few obstructions. However, it is located close to other structures and must not endager anybody nearby. As a result, a maximum rotor diameter of 1.3m has been specified.

With this limit in place, an upper limit can be placed on the power output from the turbine. Utilising Equation 3 along with the Betz limit, an air density of 1.225 kg/m^3 [8], and an average wind speed of 7.08 ms^{-1}, maximum power output is found as 145.79 W, shown in Equation 4. This is a maximum limit to the power available in average wind conditions.

$$P_{max} = 59.3\% \times \frac{1.225 \times \pi \times 0.65^2 \times 7.08^3}{2} \quad (4)$$
$$= 145.79W \quad (5)$$

Given that the turbine is currently intended to supply energy to a small, low power lighting and irrigation system inside a greenhouse, this is a significant amount of power. This does not give an indication of expected energy yield. However given the fact that the greenhouse currently has 72 Wh of installed storage, this turbine system operating anywhere near maximum output for half an hour to an hour on any given day would easily fill the storage.

In order to design blades for optimal performance, it is important to define a few more specifics of the turbine. As mentioned previously turbines are often operated as either constant or variable speed, with constant speed often utilising pitch control systems to maintain a constant RPM on the rotor. This system is to be a variable speed system, allowing the blades to be fixed. In this configuration, it is expected that TSR is held reasonably constant at a pre-defined value [4].

Efficiency increases as TSR increases, and it is generally accepted that TSR of approximately 7 is close to optimal for variable speed configurations. This is due to the fact that although higher TSR values do have better efficiency, the efficiency gain at 7 or more is negligible, and higher TSR leads to greater stress on the blades [3] [7]. Therefore, a TSR of 7 will be utilised in this design.

Finally, it is important to determine the number of blades present on the rotor. As TSR increases, the area of solidity decreases significantly [3]. Area of solidity is a measure of how much of the swept area is physically covered by blade at any one time. Therefore reducing this value leads to lower manufacturing costs and can justify a low number of blades. With a TSR of 7, area of solidity is low enough for one, two, or three blades to be an option. Generally one and two bladed designs have stability issues [1]. Efficiency does increase with blade count, however the gains after three blades are marginal [3]. Therefore, it has been decided that this turbine will initially be a three blade configuration.

B. Airfoil Catalog

Airfoil	**Special Notes**	**Reference(s)**
S833	Developed for small HAWT	[4, 9]
BW-3	Wide drag bucket	[4]
A18		[4]
SD7032	Wide drag bucket	[4]
GOE417		[4]
SG6043		[10]

TABLE I: Airfoils selected for analysis. Foils obtained via Airfoil Tools [11].

With initial rotor specifications decided, a catalog of low Reynolds number airfoils has been constructed. Initially the intention was to analyse airfoils from various sources in the literature, however while performing a search it became apparent that the work done by P. Giguere and M. Selig stands as primary work in this area. Many subsequent papers expand on their conclusions and develop proprietary airfoils that improve on standard models. These airfoils are often not public, and as such most of the foils analysed in this project are those that were identified as effective profiles for small HAWTs in that paper.

A selection of six airfoils was made, listed in Table I. Each airfoil has been chosen based on desirable glide ratio, however some airfoils are selected based on other quantifiers. Two of the airfoils have been selected based on a “wide drag bucket”. This refers to an airfoil that maintains an optimal glide ratio for a wide range of attack angles, rather than having a narrow band of angles where optimal glide ratio is achieved.

C. Airfoil Analysis

Airfoils are analysed in QBlade, an open source package for performing turbine simulation [12]. This software allows for analysis of airfoil lift/drag characteristics, along with simulation of blade performance and overall expected turbine characteristics.

Each of the airfoils in Table I has been obtained from an online database of aifoils [11]. Before proper analysis could be performed, an approximation of the operating Reynolds number for each airfoil had to be made.

In order to do this, chord length must be known. In the book *Wind Energy Explained* [1], a process for determining the varying chord length along a blade is described. Equations are derived for modelling the angle of relative wind (Equation 6), along with the chord length along the blade (Equation 7).

$$\theta_{rel} = tan^{-1}(\frac{2}{3\lambda_r}) \tag{6}$$

$\lambda_r =$ TSR at r

$$c_r = \frac{8\pi r sin\theta_{rel}}{3BC_l\lambda_r} \tag{7}$$

$c =$ Chord length at r
$B =$ Blade count
$C_l =$ Lift coefficient

Each equation calculates that parameter for a given point along the blade, at radius r. A spreadsheet has been created to implement these equations and develop a blade profile. Figure 5 shows the output of this spreadsheet for the S833 airfoil. Note the

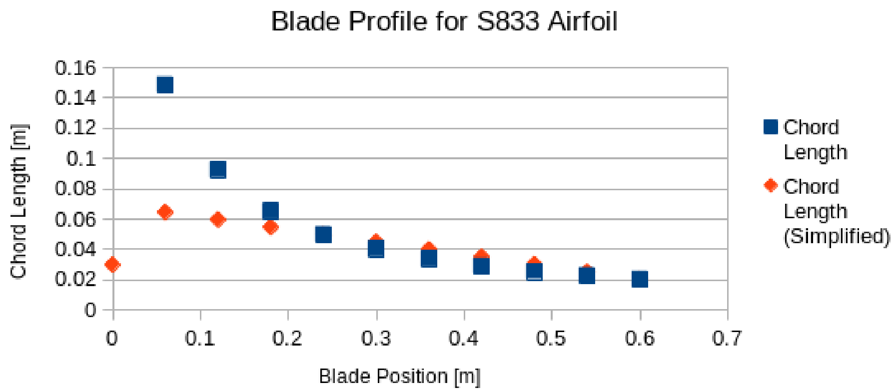

Fig. 5: Blade profile generated with the developed profile spreadsheet.

two curves, the initial chord length curve is directly from the calculation, and represents the ideal blade shape. However making a blade with such a wide root increases material costs significantly, and realistically the gains are minimal [1]. Therefore, a simplified shape has been generated based on this theoretical model, and will be used in the physical fabrication of the final blades.

Reynolds number, chord length, and expected lift coefficient are all interdependent. Therefore modelling the blade without a given starting point is exceedingly difficult. As a result of this, an interative approach was taken. For each airfoil an initial Reynolds number was selected, and used to generate a two dimensional simulation in QBlade. This yielded an optimal lift coefficient which could be input into the spreadsheet to generate a blade profile. Chord length at the halfway point of the blade was then utilised to calculate a new Reynolds number. This was used to generate another QBlade simulation and a new optimal C_l. This process was iterated until the resulting Reynolds number appeared to converge on a value, and this was taken as the Reynolds number for that airfoil in the expected average wind conditions. Table II shows these results.

With approximate Reynolds operating points, each airfoil could be simulated. Figure 6 shows a Cl vs Cd graph (drag polar) and a glide ratio to angle of attack plot. In the literature there is often reference to a “drag bucket”, this is observed in the drag polar plot as a “U” shape in the line. This represents an airfoil that maintains an optimal (minimal) drag coefficient

Airfoil	**Reynolds Number**
S833	148680
BW3	118944
GOE417	132160
A18	128856
SD7032	118944
SG6043	1024240

TABLE II: Final Reynolds number for each airfoil

over a wide range of lift coefficients. This tends to make the airfoil perform well in a wider range of conditions.

Drag polars can also be used to determine the maximum glide ratio [13], however this can be done more effectively with the glide ratio to angle of attack plot. This plot shows how glide ratio changes with angle of attack, and can be used to determine the range of angles for which the blade performs optimally. It is interesting to note that for the foils with the wider drag bucket, the glide ratio plot has a much wider peak, implying that the foil operates effectively for a wide range of attack angles. For the foils with narrower drag buckets, the glide ratio has a very sharp peak, and drops off quickly to either side.

With this in mind, three airfoils have been selected for further analysis via physical construction, and their simulation results are highlighted in Figure 7.

The A18 foil has been selected as it has the highest potential glide ratio, however it is worth noting the peak climbs to just over 70 at approximately 5° before a very sharp drop off, implying that this

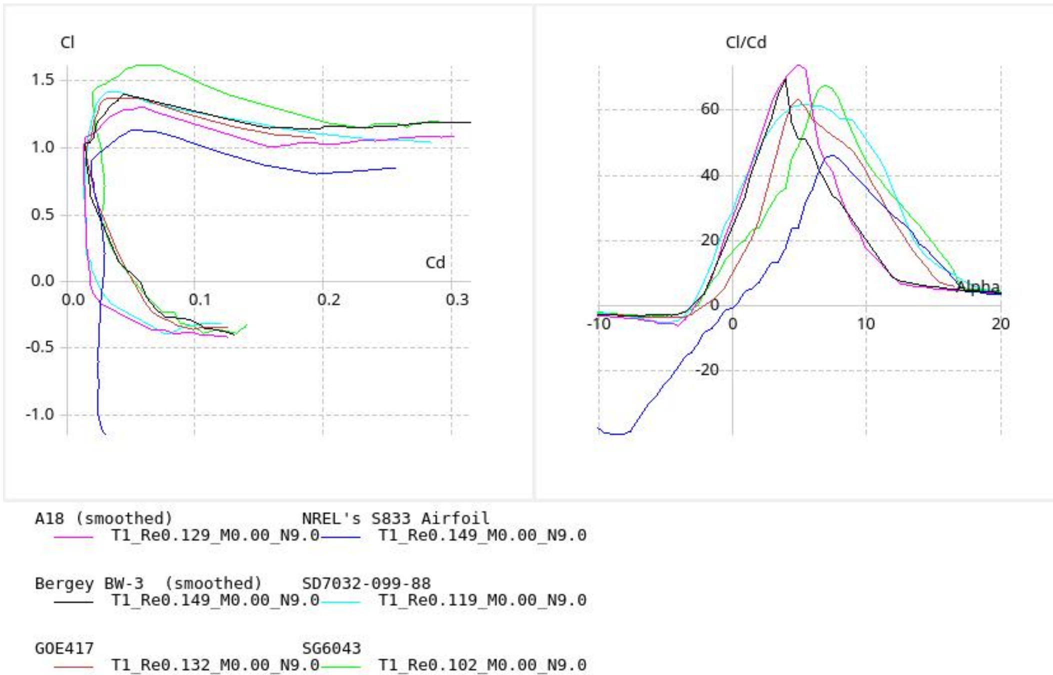

Fig. 6: QBlade airfoil simulation results.

blade will need to operate in expected conditions to function optimally. An SG6043 foil has been chosen for a similar reason, with a very high potential glide ratio. This foil also has a narrow drag bucket, however the peak is much more symmetrical. Finally, the SD7032 foil has been selected as it had the widest drag bucket of the foils analysed. This translates into a very wide range of attack angles that provide a near optimal glide ratio, likely making this blade more effective in conditions where the rotor does not maintain the expected TSR.

Figure 9 shows the developed models for each of the three proposed airfoils. Each blade will have an attachment at the base for mounting to the nacelle. This setup is roughly illustrated in Figure 8. Each blade will be physically analysed to obtain a power curve in varying windspeeds.

V. Discussion

It is important to acknowledge the fact that this design process is a very practical approach, with little in depth mathematical analysis of the system parameters. This is not necessarily a negative thing, as the presented process is arguably more straightforward than others presented in the literature. It will be important during testing to compare the power coefficient of the final turbine to that of a similar turbine designed with a more rigorous process, potentially providing insight into how much efficiency is gained by extra investment in development time.

This process does not include significant consideration around blade material. Materials are an incredibly important aspect of blade design, however for this prototyping stage it has been decided easiest to 3D print blades for analysis. Ideally blades will be fabricated in a outdoor suitable material such as ABS or PETG, however PLA will be perfectly suitable for short-term testing. This process will require printing blades in mutliple sections, and may lead to a lack of stiffness in the blades. This could result in snapping in high wind conditions, and therefore it will be important to have a process in place for testing in higher windspeed, and monitoring for signs of blade failure. If this does occur, future iterations may need to address alternative fabrication processes and materials.

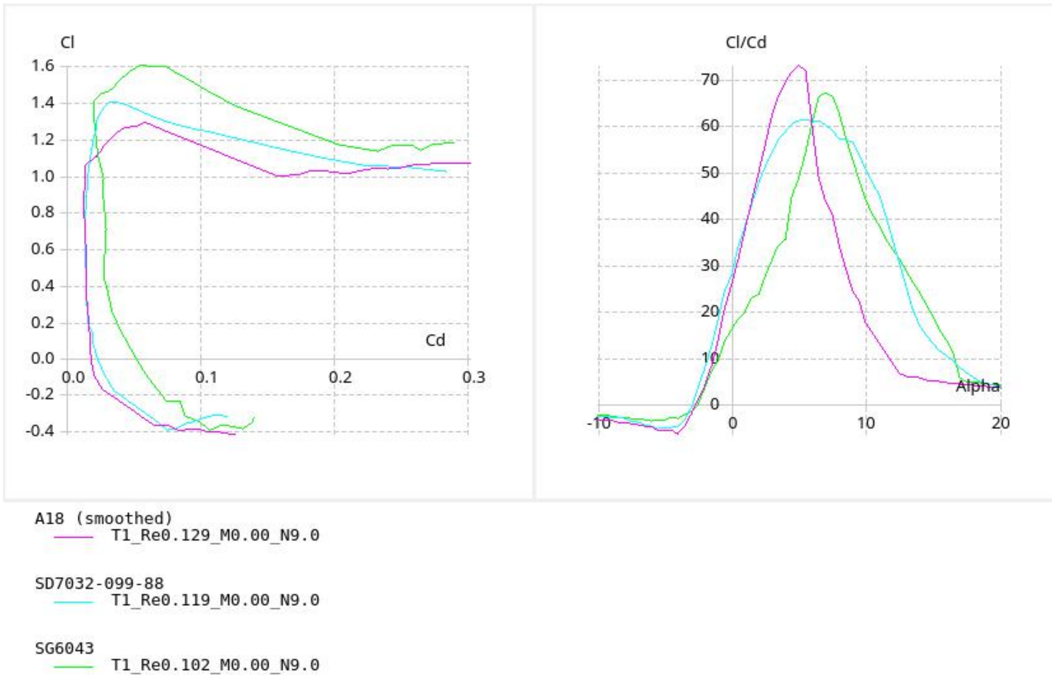

Fig. 7: QBlade airfoil simulation results for the three selected airfoils.

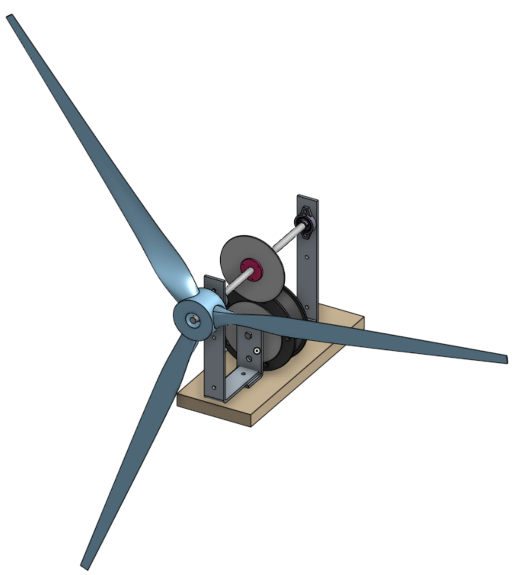

Fig. 8: Example of blades mounted on nacelle, utilising the SD7032 airfoil blades.

If blades are flimsy and cannot handle higher windspeeds, it is possible that increasing chord length could increase their strength. The selected chord lengths have been iteratively determined as the optimal chord lengths for maximum output, however through this process it became clear that chord length is relative to TSR [3]. Therefore, if thicker blades are required, a slight decrease in TSR will lead to higher ratio of solidity, and therefore thicker blades.

Many sources in the literature discuss changing the airfoil profile along the blade [1, 3]. This is done as it is beneficial to have a thicker airfoil at the root where structural integrity is more important, and torque is low, while it is important to maximise aerodynamic efficiency at the tip of the blade. This has not been done for this design, as time constraints only allowed for development and simulation with a single airfoil per blade. It would be worthwhile investigating varying airfoil for future iterations.

Finally, it is worth noting that the windspeed data utilised is only an approximate representation and does not accurately reflect the wind behaviour at the selected location. As discussed previously, future iterations on this design should install an anemometer at the location and collect accurate data over a longer

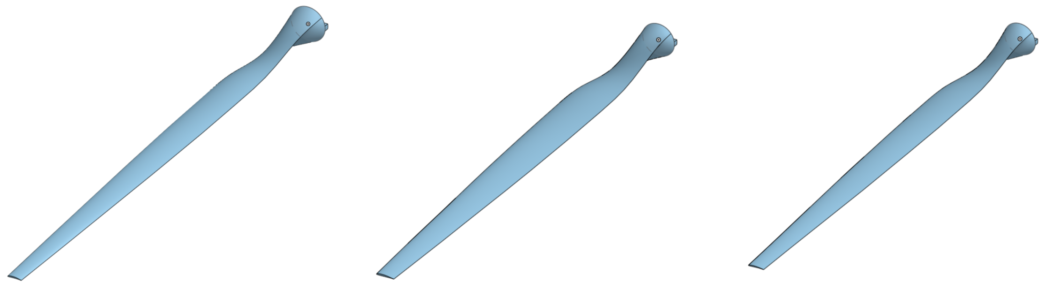

(a) SG6043 Blade Model (b) SD7032 Blade Model (c) A18 Blade Model

Fig. 9: Three blade models, developed in OnShape.

period of time.

VI. Conclusion

This report has presented a process for the development of small horizontal axis wind turbine blades. A selection of airfoils has been suggested, and analysis has been performed for expected lift characteristics. Models of the developed blades have been developed, and are to be 3D printed for physical analysis.

This design has provided a set of minimum viable blades optimised for the specified location. Further iterations on these designs should do further analysis on material selection, along with analysing the impacts of varying the airfoil along the length of the blade.

Following this design, the next steps in this project are to develop an understanding of scooter motor properties when acting as a generator, and analyse the impacts of a gearbox on its performance. Blades are to be fabricated, and mounted to the nacelle. From here, tests will be devised to develop a power output vs windspeed plot for each rotor.

References

[1] J. F. Manwell, Mac Gowan J G., and A. L. Rogers. *Wind energy explained*. John Wiley and Sons, 2002.

[2] Engineers Edge. *Viscosity of air, dynamic and kinematic*. URL: https://www.engineersedge.com/physics/viscosity_of_air_dynamic_and_kinematic_14483.htm.

[3] Peter J. Schubel and Richard J. Crossley. “Wind Turbine Blade Design”. In: *Energies* 5.9 (2012), pp. 3425–3449. URL: https://www-proquest-com.helicon.vuw.ac.nz/scholarly-journals/wind-turbine-blade-design/docview/1537075869/se-2?accountid=14782.

[4] Philippe Giguère and Michael S. Selig. “Low Reynolds Number Airfoils for Small Horizontal Axis Wind Turbines”. In: *Wind Engineering* 21.6 (1997), pp. 367–380. ISSN: 0309524X, 2048402X. URL: http://www.jstor.org/stable/43749658.

[5] Hani Muhsen, Wael Al-Kouz, and Waqar Khan. “Small Wind Turbine Blade Design and Optimization”. In: *Symmetry* 12.1 (2020). ISSN: 2073-8994. DOI: 10.3390/sym12010018. URL: https://www.mdpi.com/2073-8994/12/1/18.

[6] *NIWA Solarview*. Accessed: 08/03/2021. URL: https://solarview.niwa.co.nz/.

[7] Søren Gundtof. *Wind Turbines*. Tech. rep. University College of Aarhus, 2009.

[8] *Air - Density, Specific Weight and Thermal Expansion Coefficient at Varying Temperature and Constant Pressures*. Accessed: 08/03/2021. URL: https://www.engineeringtoolbox.com/air-density-specific-weight-d_600.html.

[9] *Wind Turbine Airfoil List*. Accessed: 03/08/2021. URL: https://wind.nrel.gov/airfoils/AirfoilList.html.

[10] N Karthikeyan and T Suthakar. “Computational studies on small wind turbine performance characteristics”. In: *Journal of Physics: Conference Series* 759 (Oct. 2016), p. 012087. DOI: 10.1088/1742-6596/759/1/012087. URL:

https://doi.org/10.1088/1742-6596/759/1/012087.

[11] *Airfoil Tools*. Accessed 04/08/2021. URL: http://airfoiltools.com/.

[12] TU Berlin Hermann Föttinger Institute. *QBlade*. URL: http://www.q-blade.org/.

[13] Martin Hepperle. *How do I read the polar digrams?* Accessed: 07/08/2021. URL: https://www.mh-aerotools.de/airfoils/hdipolar.htm.